

RESEARCH

Open Access



Assessing implant position and bone properties after cementless total knee arthroplasty using weight-bearing computed tomography

Jane Lin¹, Mariam Zamani^{2,3}, Vishal Kalia⁴, Edward M. Vasarhelyi¹, Brent A. Lanting¹ and Matthew G. Teeter^{1,2,3,4*}

Abstract

Background Weight-bearing CT (WBCT) scanners are growing in availability and provide the capability of three-dimensional imaging while a joint is under load. This may be particularly useful in relation to personalized total knee arthroplasty (TKA) with cementless implants. The objective of the present study was to evaluate the utility and inter-observer repeatability of WBCT in assessing patients with cementless TKA in a loaded position.

Methods Forty patients who underwent primary TKA approximately 3 years previously and received one of two cementless implant systems were recruited, including two subjects with bilateral TKA, for a total of 42 knees. All subjects underwent examination of their knee with WBCT while standing, thereby loading the indicated knee. Lateral distal femoral angle (LDFA), medial proximal tibial angle (MPTA), hip-knee-ankle angle (HKAA), and joint line obliquity (JLO) were measured on full length radiographs and the WBCT exams by two observers. Femoral and tibial component rotation was measured on WBCT. Greyscale values representing bone density were assessed in five identically sized regions of interests in both the femur and the tibia on WBCT.

Results Inter-observer agreement for alignment was good (95% ICC: 0.87). Inter-observer agreement for femoral component rotation was moderate (95% ICC: 0.67) and for tibial component rotation was good (95% ICC: 0.84). Inter-observer agreement for femoral greyscale values was good (95% ICC: 0.87) and for tibial greyscale values was excellent (95% ICC: 0.97).

Conclusion Cementless TKA can be assessed postoperatively using WBCT to measure implant position and bone density in a functional, loaded joint position with good inter-observer repeatability.

Keywords Cementless total knee arthroplasty, Implant fixation, Coronal alignment, Hip-knee-ankle angle, Joint line obliquity, Bone density

*Correspondence:

Matthew G. Teeter
matthew.teeter@lhsc.on.ca

¹Division of Orthopaedic Surgery, Department of Surgery, Schulich School of Medicine & Dentistry, Western University, London, ON, Canada

²Department of Medical Biophysics, Schulich School of Medicine & Dentistry, Western University, London, ON, Canada

³Robarts Research Institute, Schulich School of Medicine & Dentistry, Western University, London, ON, Canada

⁴Department of Medical Imaging, Schulich School of Medicine & Dentistry, Western University, London, ON, Canada



Introduction

The ideal positioning of components in total knee arthroplasty (TKA) remains a topic of debate [1]. Assessment of component positioning is most often performed from standing hip-to-ankle radiographs [2]. Short film radiographs can be an acceptable alternative in some instances but are not as accurate as full-length radiographs [3, 4]. Computed tomography (CT) scans enable full three-dimensional (3D) analysis of component position relative to bony anatomy [5]. CT scans also allow the assessment of peri-implant bone density [6]. However, CT scans are performed with the patient supine in the scanner bed, so that the joint is unloaded.

Recent advances in cone-beam CT (CBCT) technology have led to the development of weight-bearing CT (WBCT) scanners capable of 3D scans of joints under loading [7]. An additional benefit of this technology is reduced ionizing radiation dose compared to conventional CT [8]. WBCT has become recognized for its utility in studying knee osteoarthritis and injury to the anterior cruciate ligament [9, 10]. Cone-beam CT scanners have been used to assess patients with cemented TKA, but not with the patient in a standing position [8, 11, 12].

There are current trends towards personalized TKA that respects patients' native joint alignment and the use of cementless TKA implants that rely on bone ingrowth [13, 14]. WBCT is therefore a potentially useful tool in both the clinical and research environments to assess implant position and bone in patients receiving cementless TKA. The objective of the present study was to evaluate the utility and inter-observer repeatability of WBCT in assessing patients with cementless TKA in a loaded position for alignment, component rotation, and bone density.

Materials and methods

Ethics approval was obtained from the Western University Health Sciences Research Ethics Board in accordance with the Declaration of Helsinki. All participants provided consent to participate. Patients who had underwent primary TKA with one of two cementless implants and were at least one year post-operation were eligible for inclusion. Excluded were patients who had undergone revision of their TKA as well as those who lacked a post-operative hip-to-ankle radiograph. The two implant systems were the Triathlon Tritanium (Styker, Mahwah, NJ) and the Attune Cementless Rotating Platform (DePuy Synthes, Warsaw, IN). For each implant system, there were $n=21$ knees assessed from $n=10$ men and $n=10$ women per group, with one patient per group having bilateral TKA. Patients in the Triathlon group were recruited first and then Attune patients were subsequently recruited with matching sex, age, and

post-operative hip-knee-ankle angles. For the Triathlon group, all 21 knees were cruciate retaining. For the Attune group, $n=17$ knees were cruciate retaining and $n=4$ were posterior-stabilized. In the Triathlon group the mean age was 69 years (range, 55 to 81 years) and the mean time post-operation was 3.6 years (range, 2.6 to 5 years). In the Attune group the mean age was 67 years (range, 54 to 80 years) and the mean time post-operation was 2.9 years (range, 2.4 to 3.4 years). Data from both groups was pooled for a total of $n=42$ knees examined.

All patients received hip-knee-ankle radiographs as part of standard of care at least one year postoperation. Patients also underwent a WBCT scan in a standing, weight-bearing position on the indicated knee using a commercially available WBCT system (Onsight 3D Extremity System, Carestream Health, Rochester, NY). Scan parameters were 90kVp, exposure 20-41mAs, slice thickness 0.26 mm, increments 0.26 mm, 884 slices, a matrix of 1024×1024 , rotation time 10 s, and approximate dose 0.04-0.06mSv. Analysis of the DICOM images for the radiographs and WBCT was performed in 3D Slicer (slicer.org).

The lateral distal femoral angle (LDFA) and medial proximal tibial angle (MPTA) were measured on the radiographs [15]. The LDFA was the lateral angle formed between the femoral mechanical axis and the joint line of the distal femur, while the MPTA was the medial angle formed between the tibial mechanical axis and the joint line of the proximal tibia. The hip-knee-ankle angle (HKAA) was calculated as the difference between MPTA and LDFA. The joint line orientation (JLO) was calculated as the summation of the MPTA and LDFA angles.

Two observers assessed the WBCT images for radiolucencies at the bone-implant interface, measured HKAA and JLO, measured femoral and tibial component rotation, and measured bone density via greyscale values in regions of interest surrounding femoral and tibial components. The LDFA and MPTA were measured for the calculation of HKAA and JLO as described above. For LDFA, the femoral mechanical axis was drawn as the line between point 1 at the hip centre, and point 2 at the centre of the intercondylar fossa; the femoral joint line was the line tangential to the most distal points on the convexity of the medial and lateral femoral condyles of the femoral component. For MPTA, the tibial mechanical axis was drawn as the line between point 1 at the centre of the tibial plafond, and point 2 at the centre of the intercondylar eminence; the tibial joint line was the line parallel to the tibial plate. Femoral component rotation was measured by obtaining the angle between the trans-epicondylar axis and a line through the most posterior edge of the femoral condyles (Fig. 1a) [8]. Tibial component rotation was measured as the angle between two lines: the first through the centre of the keel, perpendicular to

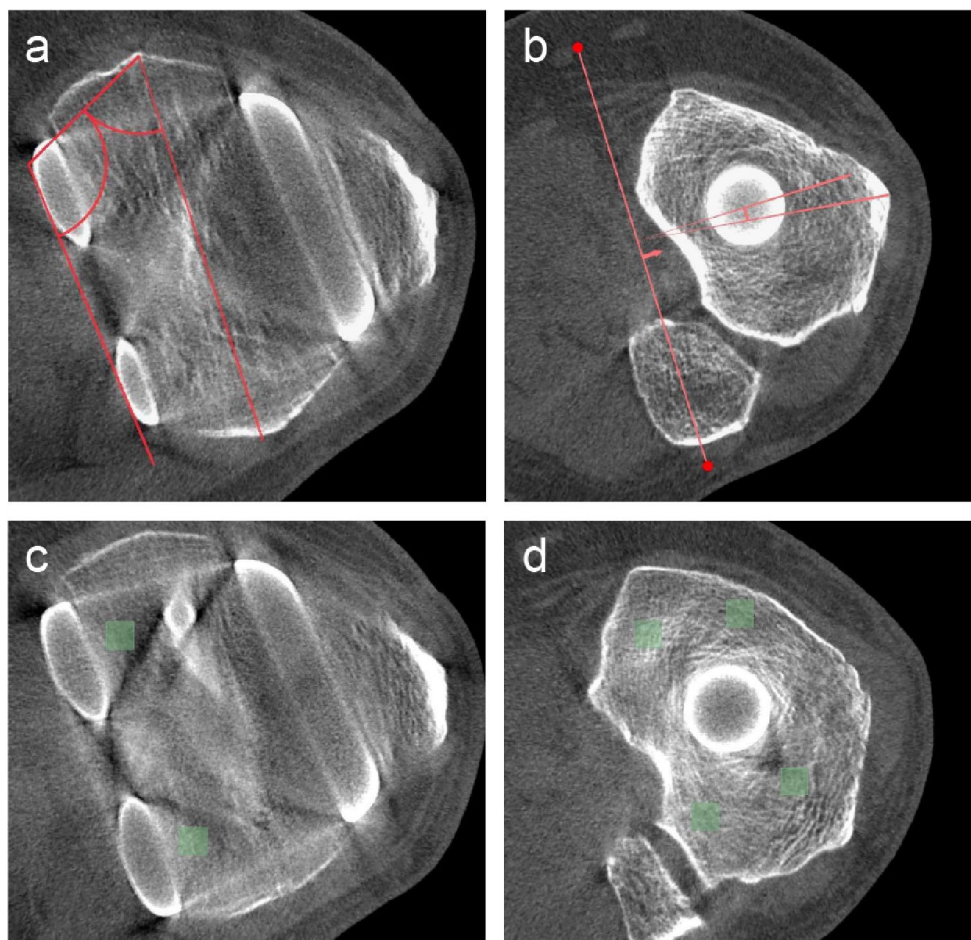


Fig. 1 Axial view of the knee joint using weight-bearing computed tomography with measurements for femoral and tibial component rotation and bone density. **(a)** Femoral component rotation. Measured by calculating two angles using the trans-epicondylar axis and a line through the posterior edge of the femoral condyles, and then subtracting their sum from 180° to determine the final rotation angle. **(b)** Tibial component rotation. Measured using the angle formed between two reference lines: the first passing through the center of the tibial keel, perpendicular to the posterior tibial plate, and the second extending from the point of intersection to the tip of the tibial tuberosity. **(c)** Femoral bone density measurement. Green boxes highlight examples of the regions of interest (ROIs) in the femur, specifically at the posterior part of the lateral and medial condyles. Bone density was assessed using greyscale values in $6\text{ mm} \times 6\text{ mm} \times 6\text{ mm}$ ROIs. **(d)** Tibial bone density measurement. Green boxes highlight examples of the ROIs in the tibia, specifically under the four pegs (anterolateral, posterolateral, posteromedial, and anteromedial). Bone density was assessed using greyscale values in $6\text{ mm} \times 6\text{ mm} \times 6\text{ mm}$ ROIs

the tangent of the posterior tibial plate, and the second line from the point of intersection of the previous perpendicular lines to the tip of the tibial tuberosity (Fig. 1b) [8]. Bone density was obtained from greyscale values in five regions each in the femur and tibia with dimensions of $6\text{ mm} \times 6\text{ mm} \times 6\text{ mm}$. Femoral regions were anterior behind the flange, above the two pegs (lateral and medial), and at the posterior part of the lateral and medial condyle (Fig. 1c). Tibial regions were under the four pegs (anterolateral, posterolateral, posteromedial, and anteromedial) and the keel of the tibial component (Fig. 1d). These regions were chosen since they were in the closest proximity to the parts of implant component responsible for fixation.

Statistical analyses were performed using Prism v9 (GraphPad, La Jolla, CA). Data normality was assessed

using the Shapiro-Wilk test. A Pearson correlation was used to determine the correlations between radiographic and WBCT measurements of MPTA, HKAA, and JLO, while a Spearman correlation was used for LDFA. A Friedman test was used to compare greyscale values between the regions of interest adjacent to the femoral and tibial components. An intraclass correlation coefficient (ICC) was calculated between observers for the WBCT measurements of LDFA, MPTA, HKAA, JLO, femoral and tibial component rotations, and femoral and tibial greyscale values.

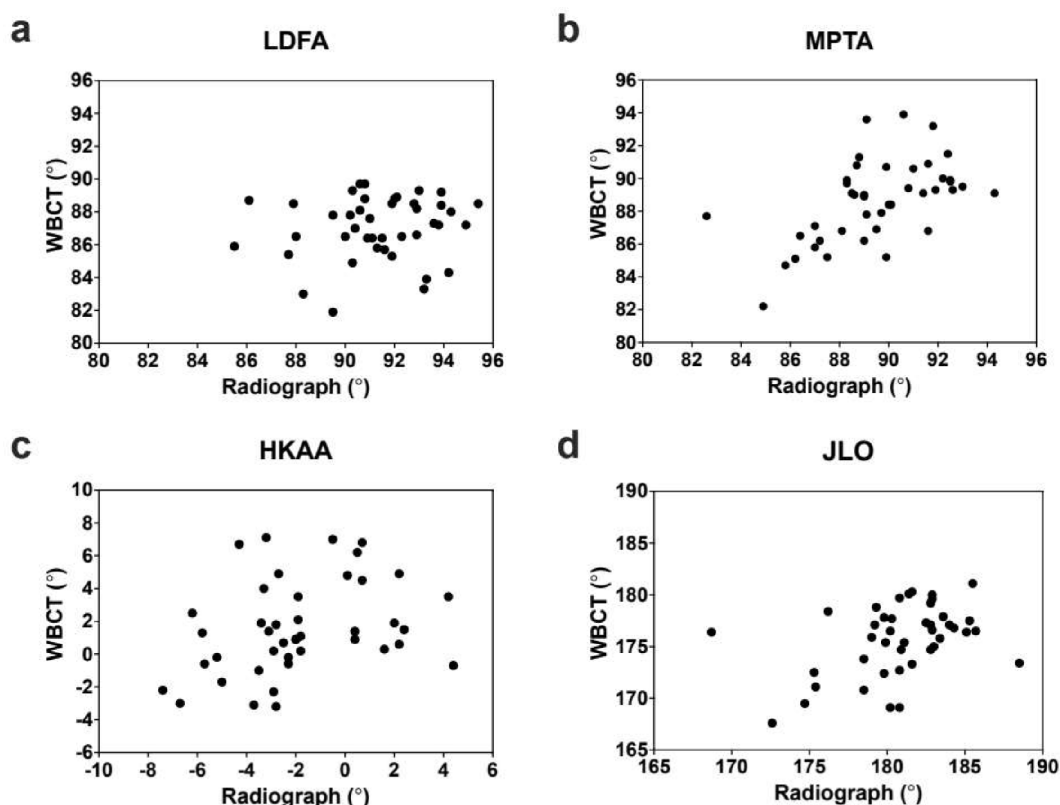


Fig. 2 Comparison of coronal plane alignment measurements between hip-knee-ankle radiographs and weight-bearing computed tomography for lateral distal femoral angle (LDFA) (a), medial proximal tibial angle (MPTA) (b), hip-knee-ankle angle (HKAA) (c), and joint line orientation (JLO) (d)

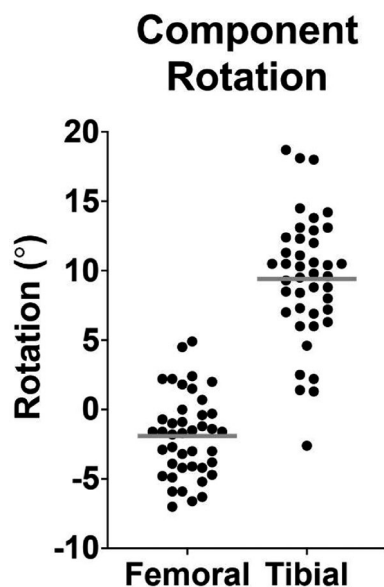


Fig. 3 Femoral and tibial component rotation measured on weight-bearing computed tomography. The grey lines represent mean values

Results

All implants appeared well-fixed on WBCT. Artifacts were common at the bone-implant interface, but no radiolucency was observed beyond what was determined

to be artifact.

Moderate correlations were found between the radiographic and WBCT measurements for MPTA ($r=0.555$, $p=0.001$, Fig. 2b), HKAA ($r=0.328$, $p=0.034$, Fig. 2c), and JLO ($r=0.405$, $p=0.008$, Fig. 2d) but not LDFA ($r=0.114$, $p=0.472$, Fig. 2a). Interobserver agreement for the alignment measurements from WBCT was good (95% ICC: 0.87).

There was a mean external rotation of 1.9° for the femoral component and mean internal rotation of 9.4° for the tibial component (Fig. 3). Interobserver agreement for the rotation measurements from WBCT was moderate for femoral component rotation (95% ICC: 0.67) and good for tibial component rotation (95% ICC: 0.84).

Bone density adjacent to the femoral component was lower in the anterior region of interest compared to the medial ($p<0.0001$), posterolateral ($p<0.001$), and posteromedial ($p<0.05$) regions (Fig. 4a). Bone density adjacent to the tibial component was lower ($p<0.05$) under the anterolateral region of interest compared to the posterolateral, posteromedial, and anteromedial regions (Fig. 4b). Bone density under the keel was also lower ($p<0.001$) than the posterolateral, posteromedial, and anteromedial regions. Good interobserver agreement was found for the femoral greyscale values (95%

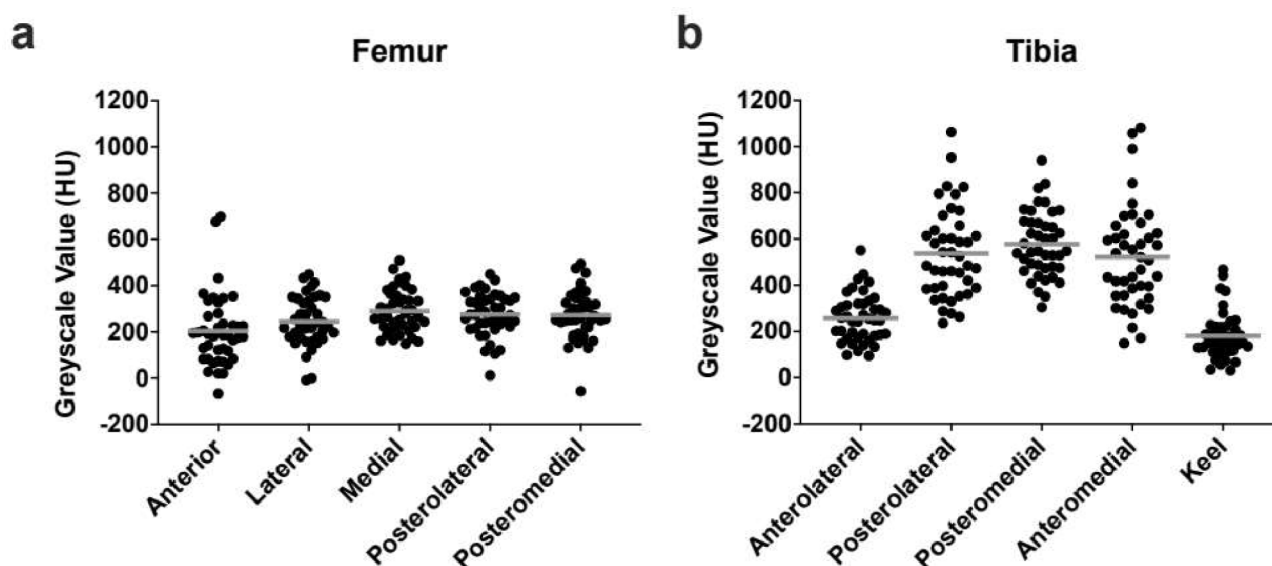


Fig. 4 Bone density represented by greyscale values from weight-bearing computed tomography in regions of interest surrounding the femoral component (a) and tibial component (b). The grey lines represent mean values

ICC: 0.87), and excellent agreement was found for tibial greyscale values (95% ICC: 0.97).

Discussion

WBCT has been reported on for studying the knee, demonstrating value in assessing joint space width, detecting osteophytes and subchondral cysts, and assessing instability following ligament injury [7, 9, 10]. However, WBCT has thus far been applied only in a limited manner to study cemented TKA [8, 11, 12]. To our knowledge, this is the first study using WBCT in a loaded, weight-bearing position to evaluate TKA patients, the first to evaluate cementless TKA, and has examined the greatest number of subjects to date. It is useful to assess WBCT in this manner given the rise in personalized TKA alignment and the use of cementless TKA fixation [13, 14]. Assessing the bone-implant interface, coronal alignment, femoral and tibial component rotation, and femoral and tibial bone density, we found good to excellent agreement between observers for all measurements.

Nardi et al. used a CBCT scanner with patients in supine position to assess 20 patients with symptomatic cemented TKA [11]. They found they were able to accurately measure femoral and tibial component rotational alignment and analyze structures with little impediment from metal artifacts. Similarly, Jaroma et al. used a CBCT scanner in non-weight-bearing position to assess 18 patients with cemented TKA prior to revision surgery for a variety of indications [12]. While our study examined a well-performing cohort and found no radiolucency beyond what could be attributed to metal artifact, the Jaroma study examined failing devices and found excellent sensitivity (97%) and good specificity

(85%) for detecting component loosening amongst their cohort. They found moderate inter-observer reliability for femoral component rotation and good reliability for tibial component rotation, as we also did in the present study. They concluded that CBCT offers a simpler imaging protocol with a lower cost and lower radiation dose to the patient than conventional CT. More recently, Dartus et al. examined 28 patients with both conventional CT and CBCT who had pain following cemented TKA [8]. While metal artifacts were noted with both CT systems, better image quality was found with CBCT, which also had a reduced radiation dose compared to conventional CT. Overall, our study of cementless TKA patients in the standing position is consistent with these three prior reports on supine scans of cemented TKA patients for metal artifact and reliability of component rotation measurements.

We observed only moderate correlations between WBCT and hip-to-ankle radiographs for measurements of MPTA, HKAA, and JLO, and no agreement for LDFA. The model of WBCT scanner used in the study was only able to scan to mid-thigh, thus the WBCT images are more comparable to short films than long leg radiographs. It has been found that short knee films are less accurate than full length radiographs for measuring HKAA [3]. Newer WBCT systems are capable of scanning from the hip to the ankle with the patient in a load-bearing position, and may be better suited to these types of measurements.

Greyscale values were lower in the femoral regions of interest compared to the tibial regions of interest. However, distal femur bone density was reported to be greater than proximal tibia bone density in patients undergoing

TKA [16]. Since the femoral component is made of dense cobalt-chromium, the femoral measurements were likely more affected by metal artifact. This is supported by the range of values in the femoral regions of interest, which fell below 0 HU in some instances, suggesting the presence of artifact. Interobserver reliability of the measurements was also better for the tibia than the femur. Together, this suggests caution is required in interpreting the greyscale values adjacent to the femoral component. In contrast, the lower tibial bone density in the anterolateral and keel regions of interest is consistent with normal anatomical variation measured previously with conventional CT [17]. The tibial components are made from porous titanium, much less dense than cobalt-chromium, and thus produce less artifact. Therefore, it is likely feasible to monitor tibial bone density adjacent to the tibial component with WBCT.

This study has several limitations. A single WBCT scanner was evaluated which may not be representative of all WBCT scanners on the market. A particular limitation of this WBCT scanner is that it can only obtain scans about the knee, rather than translate from the hip to the ankle as can be performed by other WBCT scanners available on the market. Like how short-film radiographs are less accurate than full-leg radiographs for alignment measurements [4], the knee-only WBCT used in the present study represents a worst-case accuracy compared to WBCT that can translate from hip to ankle. In contrast to prior studies only patients without any known pain or other symptoms were assessed. However, we included subjects with two common cementless TKA implant systems. Cementless implants are more recently available on the market and therefore there is a smaller population to draw from, and thus an even smaller population that would have issues following their TKA. A bone mineral density calibrator was not included in the scans, thus measurement accuracy cannot be verified, however opportunistic screening in CT scans without calibrators is becoming common [18]. Further, WBCT can distinguish anatomical differences in bone mineral density [19]. Neither was the accuracy of limb alignment assessed, only inter-observer repeatability.

In conclusion, standing WBCT has excellent potential in evaluating patients with cementless TKA, with good to excellent measurement repeatability across metrics encompassing limb alignment, component rotation, and bone density. WBCT is noted to be cost effective in orthopaedic practices and offers reduce radiation dose to patients [20]. Further applications of WBCT that include hip to ankle scans and scans in multiple positions (i.e. loaded versus unloaded or extended versus flexed) could make WBCT even more useful in assessing patients following TKA. As this study reflects measurement repeatability and not measurement accuracy, future studies

should also consider the accuracy of implant position and bone density measurements adjacent to the implant using WBCT. This might be accomplished via a three-way comparison between long-leg radiographs, hip to ankle conventional supine CT, and hip to ankle WBCT, with both CT and WBCT including bone density calibrators.

Acknowledgements

None.

Author contributions

J.L. and M.T. wrote the main manuscript text. J.L. and M.Z. acquired and analyzed the data. All authors reviewed and edited the manuscript.

Funding

Stars Career Development Award (22–0000000053) from the Arthritis Society of Canada.

Data availability

Data from this study is not publicly available due to restrictions by the local ethics research board.

Declarations

Ethics approval and consent to participate

Ethics approval was obtained from the Western University Health Research Ethics Board (#120573) in accordance with the Declaration of Helsinki. All participants provided informed consent.

Consent for publication

Not applicable.

Competing interests

The authors declare no competing interests.

Received: 27 August 2024 / Accepted: 2 May 2025

Published online: 15 May 2025

References

1. Hirschmann MT, von Eisenhart-Rothe R, Graichen H, et al. Neutrality, normality, abnormality and pathology in coronal knee alignment: why and how should we define it in the era of personalised medicine? *Knee Surg Sports Traumatol Arthrosc.* 2024;32(3):515–7. <https://doi.org/10.1002/ksa.12107>.
2. Hirschmann MT, Khan ZA, Sava MP, et al. Definition of normal, neutral, deviant and aberrant coronal knee alignment for total knee arthroplasty. *Knee Surg Sports Traumatol Arthrosc.* 2024;32(2):473–89. <https://doi.org/10.1002/ksa.12066>.
3. Park A, Stambough JB, Nunley RM, Barrack RL, Nam D. The inadequacy of short knee radiographs in evaluating coronal alignment after total knee arthroplasty. *J Arthroplasty.* 2016;31(4):878–82. <https://doi.org/10.1016/j.arth.2015.08.015>.
4. Alzahrani MM, Wood TJ, Somerville LE, Howard JL, Lanting BA, Vasarhelyi EM. Correlation of short knee radiographs and Full-length radiographs in patients undergoing total knee arthroplasty. *J Am Acad Orthop Surg.* 2019;27(11):e516–21. <https://doi.org/10.5435/JAAOS-D-18-00272>.
5. Fontalis A, Luyckx T, Vanspauwen T, et al. Strong correlation between standing Long-Leg radiographs and CT scans in measuring coronal knee alignment. *J Bone Joint Surg Am Published Online May.* 2024;13. <https://doi.org/10.2106/JBJS.23.01092>.
6. Reilly K, Munro J, Pandit S, Kress A, Walker C, Pitto RP. Inter-observer validation study of quantitative CT-osteodensitometry in total knee arthroplasty. *Arch Orthop Trauma Surg.* 2007;127(8):729–31. <https://doi.org/10.1007/s00402-007-0351-6>.
7. Segal NA, Li S. WBCT and its evolving role in OA research and clinical practice. *Osteoarthritis Imaging.* 2022;2(3–4):100083. <https://doi.org/10.1016/j.jostima.2022.100083>.

8. Dartus J, Jacques T, Martinot P, et al. The advantages of cone-beam computerised tomography (CT) in pain management following total knee arthroplasty, in comparison with conventional multi-detector CT. *Orthop Traumatology: Surg Res.* 2021;107(3). <https://doi.org/10.1016/j.otsr.2021.102874>.
9. Leão RV, Zelada SRB, Lobo CFT, et al. Assessment of knee instability in ACL-injured knees using weight-bearing computed tomography (WBCT): a novel protocol and preliminary results. *Skeletal Radiol* Published Online. 2024. <https://doi.org/10.1007/s00256-024-04562-1>.
10. Fritz B, Fritz J, Fucentese SF, Pfirrmann CWA, Sutter R. Three-dimensional analysis for quantification of knee joint space width with weight-bearing CT: comparison with non-weight-bearing CT and weight-bearing radiography. *Osteoarthritis Cartilage.* 2022;30(5):671–80. <https://doi.org/10.1016/j.joca.2021.11.019>.
11. Nardi C, Buzzi R, Molteni R, et al. The role of cone beam CT in the study of symptomatic total knee arthroplasty (TKA): A 20 cases report. *Br J Radiol.* 2017;90(1074). <https://doi.org/10.1259/bjr.20160925>.
12. Jaroma A, Suomalainen JS, Niemitukia L, Soininvaara T, Salo J, Kröger H. Imaging of symptomatic total knee arthroplasty with cone beam computed tomography. *Acta Radiol.* 2018;59(12):1500–7. <https://doi.org/10.1177/0284185118762247>.
13. Vendittoli PA, Riviere C, Hirschmann MT, Bini S. Why personalized surgery is the future of hip and knee arthroplasty: a statement from the personalized arthroplasty society. *EFORT Open Rev.* 2023;8(12):874–82. <https://doi.org/10.1530/EOR-22-0096>.
14. Martin DP, Rossi DM, Bukowski BR, et al. Mode of fixation and survivorship in primary total knee arthroplasty in the American joint replacement registry. *J Arthroplasty.* 2024;39(8):2014–21. <https://doi.org/10.1016/j.arth.2024.02.068>.
15. MacDessi SJ, Griffiths-Jones W, Harris IA, Bellemans J, Chen DB. Coronal plane alignment of the knee (CPAK) classification. *Bone Joint J.* 2021;103–B(2):329–37. <https://doi.org/10.1302/0301-620X.103B2.BJJ-2020-1050.R1>.
16. Borchardt G, Nickel B, Andersen L, et al. Femur and tibia BMD measurement in elective total knee arthroplasty candidates. *J Clin Densitom.* 2022;25(3):319–27. <https://doi.org/10.1016/j.jocd.2022.01.004>.
17. Lee YS, Nam SW, Hwang CH, Lee BK. Computed tomography based evaluation of the bone mineral density around the fixation area during knee ligament reconstructions: clinical relevance in the choice of fixation method. *Knee.* 2012;19(6):793–6. <https://doi.org/10.1016/j.knee.2012.02.011>.
18. Sebro R, Elmahdy M. Machine learning for opportunistic screening for osteoporosis and osteopenia using knee CT scans. *Can Assoc Radiol J.* 2023;74(4):676–87. <https://doi.org/10.1177/08465371231164743>.
19. Waungana TH, Qiu K, Tse JJ, et al. Accuracy of volumetric bone mineral density measurement in weight bearing, cone beam computed tomography. *J Clin Densitom.* 2024;27(3):101504. <https://doi.org/10.1016/j.jocd.2024.101504>.
20. Alexander NB, Sarfani S, Strickland CD, et al. Cost analysis and reimbursement of weightbearing computed tomography. *Foot Ankle Orthop.* 2023;8(1). <https://doi.org/10.1177/24730114231164143>.

Publisher's note

Springer Nature remains neutral with regard to jurisdictional claims in published maps and institutional affiliations.